Thermosetting Polyurethane Multiwalled Carbon Nanotube Composites

Caroline McClory,[1] Tony McNally,[1] Gerard P. Brennan,[2] James Erskine[3]

[1]*School of Mechanical and Aerospace Engineering, Queen's University Belfast, Belfast BT9 5AH, United Kingdom*
[2]*School of Biological Sciences, Medical Biology Centre, Queen's University Belfast, Belfast BT9 7BL, United Kingdom*
[3]*Hamilton-Erskine Limited, Ballygowan, Newtownards BT23 6JQ, United Kingdom*

Received 6 October 2006; accepted 23 December 2006
DOI 10.1002/app.26144
Published online 9 April 2007 in Wiley InterScience (www.interscience.wiley.com).

ABSTRACT: Thermosetting polyurethane (PU) multiwalled carbon nanotube (MWCNT) nanocomposites at loadings up to 1 wt % were prepared via an addition polymerization reaction. The morphology of the nanocomposites and degree of dispersion of the MWCNTs was studied using a combination of scanning electron microscopy (SEM), high resolution transmission electron microscopy (HRTEM) and wide angle X-ray diffraction (WAXD), and revealed the nanotubes to be highly dispersed in the PU matrix. Addition of just 0.1 wt % MWCNTs resulted in significant enhancements in stiffness, strength and toughness. Increases in Young's modulus, % elongation at break and ultimate tensile strength of 561, 302 and 397% were measured for the nanocomposites compared to the unfilled PU. The effect of the MWCNTs on the modulus of the PU was evaluated using the Rule of Mixtures, Krenchel and Halpin-Tsai models. Only the Halpin-Tsai model applied to high aspect ratio nanotubes was in good agreement with the modulus values determined experimentally. Strong interfacial shear stress was found between PU chains and nanotubes, up to 439 MPa, calculated using a modified Kelly-Tyson model. Evidence for strong interfacial interactions was obtained from the Raman spectra of both the precursor materials and nanocomposites. When the MWCNTs were added to the isophorone diisocyanate an up-shift of 14 cm^{-1} and on average 40 cm^{-1} was obtained for the position of the carbon-hydrogen (C—H) out-of plane bending (766 cm^{-1}) and isocyanate symmetric stretch (1420 cm^{-1}) modes respectively. Moreover, an up-shift of 24 cm^{-1} was recorded for the nanotube tangential mode (G-band) for the 1.0 wt % nanocomposite because of the compressive forces of the PU matrix acting on the MWCNTs. The dynamic mechanical (DMA) properties of the PU thermoset and the nanocomposites were measured as a function of temperature. J Appl Polym Sci 105: 1003–1011, 2007

Key words: polyurethanes; carbon nanotubes; nanocomposites; mechanical properties; Raman spectroscopy

INTRODUCTION

The unique properties of carbon nanotubes (CNTs) and the technological possibilities that CNT/polymer composites offer, including enhanced electrical, thermal, and mechanical properties continues to attract global research interest.[1–7] The literature to date has focused on the methods of distribution and dispersion of the CNTs within the polymer matrix and how the interaction of the polymer chains and CNTs can be promoted. Melt-mixing,[5,8] solution-casting,[6] and *in situ* polymerization[9] have all been employed for CNT-polymer composite synthesis. Nanotube dispersion can also be aided by low-impact ball milling,[10] the use of surfactants,[11] ultrasonic vibration,[12,13] and surface functionalisation by means of acid[14] or plasma[15] treatments. The vast majority of literature has reported on thermoplastic/CNT composite materials, including some very recent review articles,[16,17] but to a much lesser extent on thermoset-CNT composites, somewhat surprising as thermosets account for 25% of the global market of all natural and synthetic polymeric materials. The majority of thermoset-CNT studies have focused on epoxy- and thermosetting polyimide-CNT composites.

In particular, the electrical properties of CNT filled epoxies have been investigated. Sandler et al.[18,19] and Martin et al.[20] reported improved electrical conductivity of about 9 orders of magnitude compared to the neat resin for percolation thresholds well below 0.05 wt % CNTs. Moreover, Martin et al. also demonstrated a correlation between mean nanotube length and reduced percolation threshold, in that shorter more mobile nanotubes accelerate the rate of network formation resulting in a lower percolation threshold, at least for the epoxy system used in their study. Barrau et al.[21] studied the AC and DC conductivities of a CNT filled bisphenol A type epoxy resin as a function of temperature. They showed a DC conductivity percolation at 0.3 wt % and suggest that the main mechanism for conduction is by electron tunnelling. Gojny et al.[22] examined the effect of nanotube type and functionality on electrical conductivity and concluded that

Correspondence to: T. McNally (t.mcnally@qub.ac.uk).

any form of functionalisation that results in a decrease in aspect ratio of the nanotube yields an increased percolation threshold.

The use of high modulus, strength, and aspect ratio carbon nanotubes for mechanical reinforcement of polymers has been the subject of numerous studies. Theoretically, reinforcement on the nano-scale should provide significant enhancements in a combination of stiffness (modulus), strength, and toughness; however, to date limited improvements in all these properties for both thermoplastic and thermosetting-CNT composites have been reported. For CNT-epoxy systems, increases in modulus and tensile strength of no more than 30% are typical,[23–27] more often than not a diminution in strength and elongation at break (related to toughness) are obtained. Bai[28,29] did achieve up to a 200% increase in modulus for a CNT filled (0.1–4 wt %) epoxy system, but modest improvements in tensile strength and dramatic fall in fracture strain. The mechanical reinforcement of polymers is controlled by the degree of dispersion and orientation of CNTs in the polymer matrix, the aspect ratio of the CNTs and the efficiency of stress transfer at the interface between CNTs and polymer chains. The mechanisms for the latter are not well understood, but include chemical bonding, van der Waal type attractive forces and mechanical interlocking across the length scales. Specifically with regard to CNT reinforcement of thermosets, other factors such as the effect of CNTs on the crosslink density, cure kinetics, polymer chain mobility (thus glass transition process), and nanotube flexibility are also important factors. Additionally, chemical reaction between reactive thermoset precursors and CNTs can provide a route for the formation of a 3D network for effective stress transfer.

The influence of fluorinated and amine functionalised CNTs on the glass transition temperature (T_g) of different epoxy systems (type F and A) was investigated using dynamic mechanical analysis by Miyagawa and Drzal[7] and Gojny and Schulte[30] respectively. In the latter study the authors reported an increase in T_g with increasing CNT loading to 0.8 wt %, the effect being greater for amine-functionalised CNTs compared with nonfunctionalised CNTs, and this they concluded was a consequence of the improved interfacial interactions between nanotube and polymer. Conversely, Miyagawa and Drazl obtained significant decreases in T_g, 30°C for a CNT loading of 0.2 wt %, because of the nonstoichiometry of the epoxy matrix caused by the fluorine groups on the surface of the CNTs.

The fundamental properties of CNT filled epoxy composites for several other technologies have also been examined, including magnetic susceptibility[9] and thermal conductivity.[31] Many properties of epoxy-CNT composites can be enhanced by alignment of CNTs during processing. Martin et al.[32] used both AC and DC electric fields to induce alignment of CNT networks in an epoxy matrix; however, whereas AC fields yielded more uniform and aligned networks than DC fields, the network efficiency was not improved. Choi et al.[33] demonstrated that magnetic field processing, using fields up to 25 T and temperatures of 60°C can enhance both electrical and thermal conductivity of a 3 wt % CNT filled epoxy. As it is obvious that addition of CNTs to epoxy resins alters the cure kinetics of the reaction, and thus physical properties of the resin, surprisingly few studies on the subject have been published. Puglia at al.[34] using a combination of thermal analysis and Raman spectroscopy showed that single walled carbon nanotubes (SWCNTs) can act as a strong catalyst for a relatively highly loading (>5 wt %) epoxy resin. The incorporation of CNTs into thermosetting polyimides has also been studied by Jiang et al.[13] and Ogasawara et al.[35]

In this article, we report the preparation of MWCNT filled thermosetting polyurethane (PU) resins and examine the morphology and degree of dispersion of MWCNTs in these composites using a combination of microscopy techniques and X-ray diffraction. The tensile and dynamic mechanical properties of the composites are measured and evidence is provided from Raman spectroscopy for both chemical and physical interactions between the CNTs and resin, which in part help explain the significant improvements in stiffness, strength and toughness obtained on addition of MWCNTs to the PU resin.

EXPERIMENTAL

Materials

The thermoset PU used in the study was a two part rigid polyurethane system consisting of an isophorone diisocyanate and a polyetherpolyol, kindly supplied by Kommerling GmbH, Langelsheim, Germany. The multiwalled carbon nanotubes (MWCNTs) were supplied by Sun Nanotech, People's Republic of China. The MWCNTs were prepared by a chemical vapor deposition (CVD) process using acetylene as the carbon source and Fe and Ni as supporting catalysts. The final product, after purification, yielded MWCNTs >85% pure having diameters within the range 10–30 nm and average lengths between 1 and 10 μm.

Nanocomposite preparation

The schematic diagram in Figure 1 illustrates the nanocomposite preparation regime adopted. The polyurethane precursors were degassed for at least 8 h before processing in a vacuum oven at −1.0 mbar vacuum pressure. The MWCNTs were dried for at least 8 h at 80°C. Loadings of 0.1 and 1.0 wt %. MWCNTs

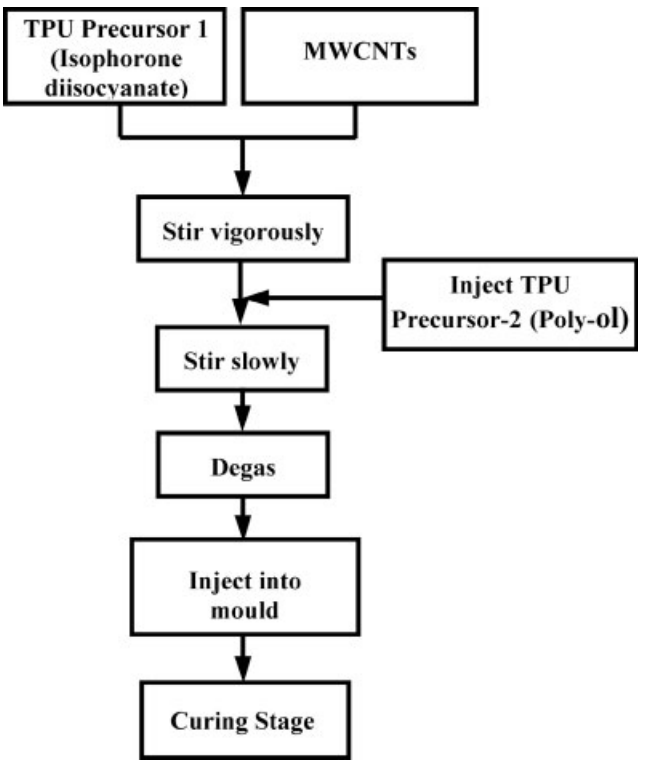

Figure 1 Schematic diagram of the synthesis route for MWCNT filled thermoset PU.

were added directly to the isophorone diisocyanate. Using a three port round bottom reaction flask, the MWCNTs were admixed and sheared using a high shear mechanical mixer set at a rotor speed of 500 rpm for 90 min. A constant vacuum was applied to degas and to keep the mixture as dry as possible during processing, as both precursors are extremely hygroscopic. The second precursor (polyetherpolyol) was slowly injected into the reaction flask through a sealed opening and stirred slowly for a further 10 min. The mixture was then allowed to rest under vacuum for a short time to minimize foam and bubble formation before removal. Samples for mechanical testing were produced by injecting the liquid mix into predried PTFE molds, machined to standard test dimensions according to tensile test requirements detailed in BS EN ISO 527-2:1996.

Characterization

The morphology and level of dispersion of MWCNTs in the PU was investigated using a combination of SEM, HRTEM, and XRD. Samples for SEM were prepared by cryogenic fracture after immersion in liquid nitrogen and subsequent sputtering of gold. These samples were then imaged using a Leo Supra-25 thermal field emission SEM with an operating voltage of 20 kV. Specimens (90 nm thick) for TEM examination were microtomed using a diamond knife from molded samples using an Ultracut-E Reichert Jung ultramicrotome. TEM characterization was carried out using an FEI Tecnai F20 field emission high-resolution transmission electron microscope using an accelerating voltage of 200 kV. Wide Angle X-Ray Diffraction spectra (WAXD) of the PU/MWCNT composites and MWCNTs were recorded using a PANalytical X'Pert Pro Siemens D5000 diffractometer using Cu-K_α radiation ($\lambda = 1.5406$ Å). The scanning rate was 1° min^{-1} in the 2θ range of 1–40°. Raman spectra were collected using an Avalon Instruments Raman Station R1 fitted with an 8200 Detector Element Echelle CCD detector. The system was capable of collecting spectra over a Raman shift spectral range of $\sim$ 250–3500 cm^{-1}. The mechanical properties of molded samples were measured using an Instron 4411 Universal Tester with a 100 N load cell. All tests were conducted at the ambient temperature using a crosshead speed of 50 mm min^{-1}. Ten specimens of each composite were tested according to BS EN ISO 527-2:1996 (Annex A). DMA measurements were performed using a Perkin-Elmer Dynamic Mechanical Analyser, model DMA-1, operating in a dual cantilever multi-frequency mode, using a scan rate of 3°C min^{-1} in the range from -100 to 140°C.

RESULTS AND DISCUSSION

The morphology and degree of dispersion of the MWCNT filled PU matrix was investigated using a combination of SEM, TEM and WAXD. Figures 2(a,b) show SEM images of 0.1 and 1.0 wt % MWCNT nanocomposites respectively, which are representative of their microstructure and show the MWCNTs are highly dispersed, somewhat disentangled, uniformly distributed and randomly oriented across the entire PU matrix. Even after severe cryo-fracturing of the test specimens, few if any voids were evident, suggesting strong interfacial interactions between the nanotubes and PU resin. Moreover, the average diameter of the CNTs has increased from about 10–30 nm prior to mixing with the resin to greater than 50 nm after curing, further evidence for good surface wetting and thus good interfacial adhesion between the PU and MWCNTs. Schadler et al.[24] described a similar morphology for MWCNTs embedded in an epoxy matrix as being 'curved and interwoven in the composite', which suggested extreme flexibility. The nanotubes appear to form interconnecting bridge structures at points along the freeze-fractured surface between the polymer/nanotube interfaces, facilitating a load transfer mechanism for CNT reinforcement of polymers.[36] The MWCNTs protruding from the PU matrix as well as being coated by resin are embedded in the polymer matrix providing resistance to the fracture force and reinforce the polymer. High speed me-

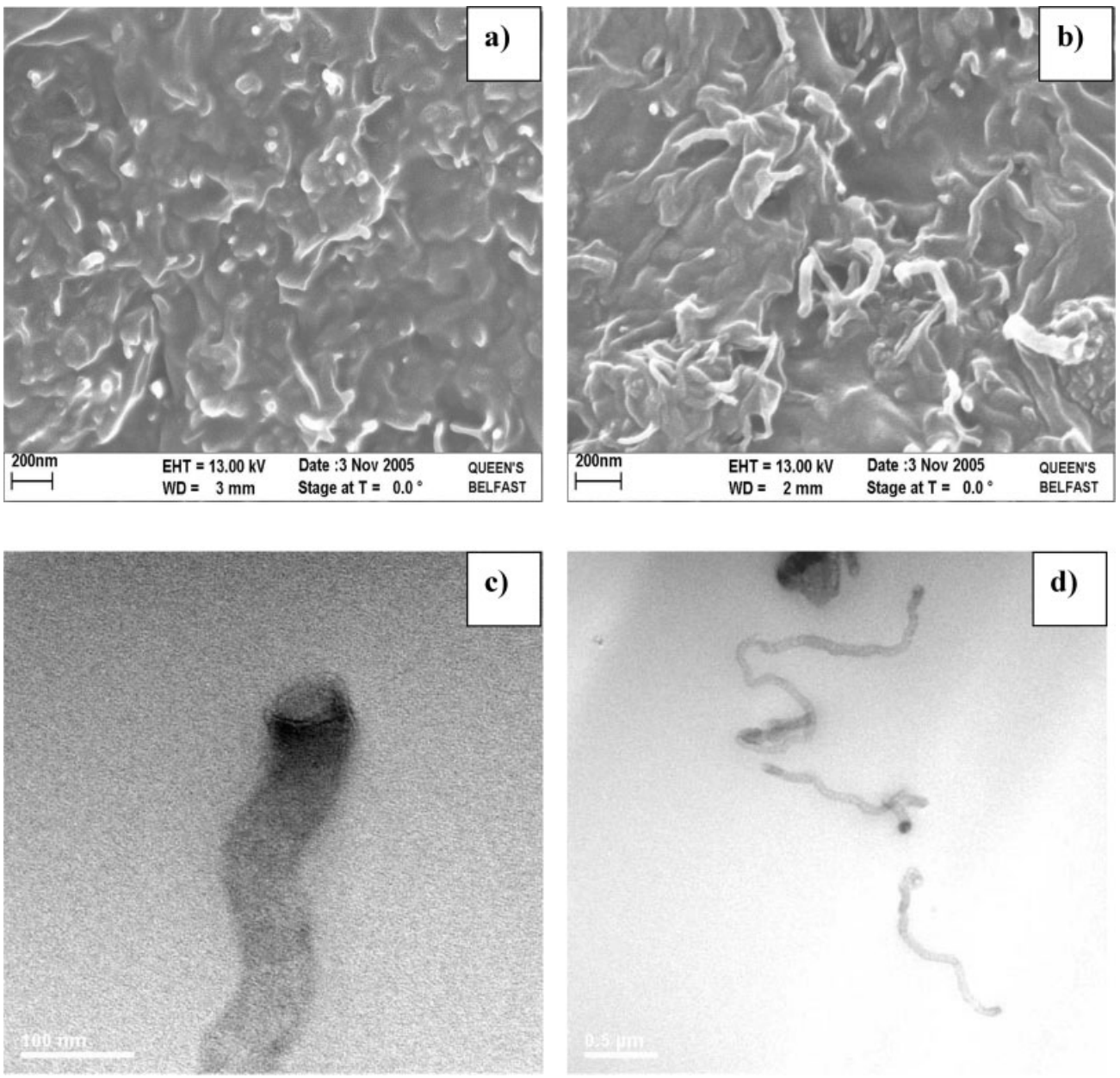

Figure 2 SEM images of (a) cryo-fractured surface of PU/$MWCNT_{0.1}$ nanocomposite, (b) cryo-fractured surface of PU/$MWCNT_{1.0}$ nanocomposite, (c) TEM of PU/$MWCNT_{0.1}$, and (d) TEM of PU/$MWCNT_{0.1}$ nanocomposite showing a number of unraveled and elongated MWCNTs.

chanical stirring during nanocomposite preparation aids disentanglement and causes fragmentation of the CNTs, as shown in Figure 2(c,d). The nanotubes used in this study had average lengths between 1 and 10 μm prior to mixing, but many sub 1 μm length tubes were observed by HRTEM. Further evidence of a high degree of dispersion of MWCNTs within the polyurethane matrix was obtained from WAXD measurements, see Figure 3. The characteristic sharp diffraction peak for MWCNTs which occurs at a scattering angle of $2\theta = 26^\circ$ is derived from the ordered arrangement of the concentric cylinders of graphitic carbon[37] and has disappeared for the composites prepared. The shear forces achieved during mixing manifests in tearing and pulling of the MWCNTs thus destroying the short range order of the concentric geometry of MWCNTs.

The tensile properties, Young's modulus, ultimate tensile strength (U.T.S.) and percentage elongation at break of the pure PU resin and PU/MWCNT composites were recorded and are shown in Figure 4. The Young's modulus of PU resin increased by 97 and 561% from 6.4 to 12.6 to 42.34 MPa on the addition of 0.1 wt % and 1 wt % MWCNTs respectively. Concomitantly, the U.T.S. of the PU/MWCNT composites increased by about 397% when either 0.1 or 1 wt %

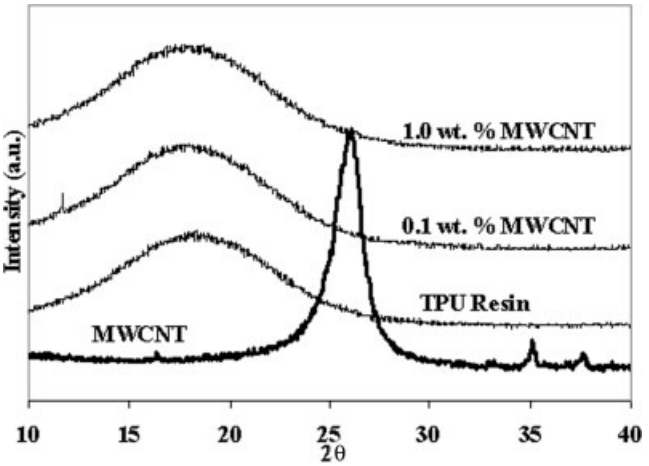

Figure 3 X-ray diffraction patterns for PU resin, MWCNTs, and PU/MWCNT nanocomposites.

MWCNTs were mixed with the neat PU resin. Furthermore, the percentage elongation at break (relative measure of toughness) of the resin increased from 83 to 302% on the addition of just 0.1 wt % nanotubes, then decreased slightly when 1.0 wt % MWCNTs was added to 272%, compared to the virgin thermoset material. The combination and magnitude of these simultaneous improvements in Young's modulus, U.T.S and elongation at break are indicative of a nano-scale reinforcement. These enhancements in mechanical properties can be attributed firstly to the outstanding physical properties of the MWCNTs, e.g., high aspect ratio, high strength, and secondly to the high dispersion of MWCNTs throughout the polymer matrix and good interfacial interaction between materials. The increased modulus and ultimate tensile strength are indications of good load transfer from the matrix to the tubes. The improved strain behavior of the composites may be explained by a sliding or telescopic mechanism reported by Pötschke et al.[5] in that polymer resin ingresses into the nanotube structure and under load is consequentially further reinforced by this sliding mechanism. Here, we reported dramatically increased strain at break coupled with increased tensile strength, achievable as the MWCNTs are uniformly dispersed within the PU resin and strong interfacial adhesion exists between the nanotubes and resin. The interfacial shear stress, τ_{NT}, can be determined using a modified form of the Kelly-Tyson model, expressed as

$$\tau_{NT} = \frac{\sigma_{NT}}{2\left(L_c/D\right)}\left(1 - \frac{d^2_{NT}}{D^2_{NT}}\right) \quad (1)$$

where σ_{NT}, L_c, d, and D are the failure stress, critical length, inner and outer diameter of the CNTs, respectively. The MWCNTs used in this study had an average inner and outer diameter of 3.7 and 23.6 nm, determined from examination of TEM images, aspect ratios ranging from 1000 down to 33 and the subsequent interfacial shear stress was calculated to be between 14.7 and 439 MPa. These values provide convincing evidence that strong interfacial adhesion exists between CNTs and the PU resin, and are comparable to what has been reported for other CNT/polymer systems.[25,38,39] Furthermore, the work done in pulling a nanotube from a polymer matrix is related to the interfacial shear stress by

$$W = \pi r\, \tau_{NT} L^2 \quad (2)$$

where W is the total work done, r is the outer radius and L the length of the carbon nanotube. W was determined to be in the range 3.26×10^{-12}–1.09×10^{-9} J for the MWCNTs added to the PU resin. The latter value

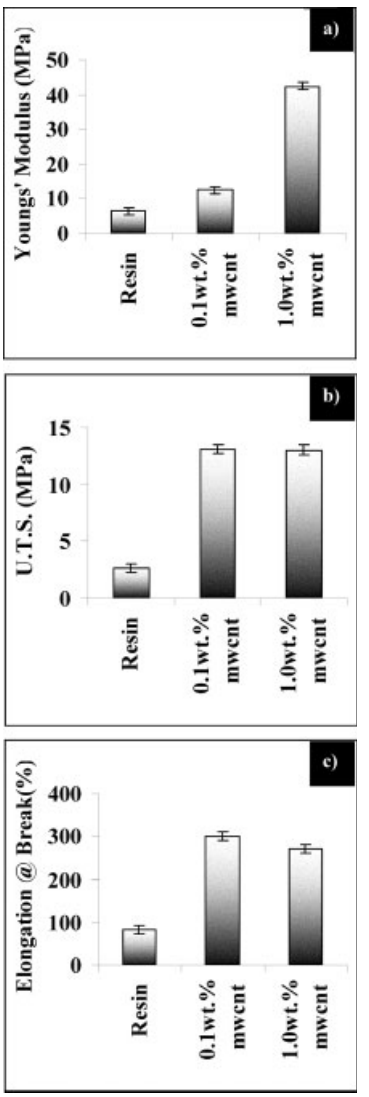

Figure 4 Mechanical properties of TPU/MWCNT nanocomposites, (a) Young's modulus, (b) ultimate tensile strength (U.T.S.), and (c) % elongation at break.

TABLE I
Comparison of the Modulus Values Measured Experimentally with Those Calculated from Models

Composite (wt %)	E_{exp} (MPa)	E_N	E_{RM} (GPa)	E_{KM} (GPa)	E_{HT} ζ_{low} (MPa)	E_{HT} ζ_{med} (MPa)	E_{HT} ζ_{high} (MPa)
0.1	12.6	2.0	0.21	0.21	2.53	7.34	10.16
1.0	42.3	6.6	2.03	2.01	7.66	15.95	44.64

E_N, $E_{composite}/E_{matrix}$; RM, rule of mixtures; KM, Krenchel model; HT, Halpin-Tsai model low, medium, and high refer to aspect ratio.

is 4 orders of magnitude greater than that reported previously for an epoxy/MWCNT composite.[39]

The values obtained experimentally for Young's modulus of the nanocomposites were compared to those calculated from models used to describe short-fiber reinforcement of polymers, see Table I. In the simplest form, the modulus of composites with randomly oriented fibers (nantotubes) can be described using the 'rule of mixtures' law, given by

$$E_{comp} = \alpha V_f E_f + (1 - V_f)E_m \quad (3)$$

and

$$E_f = (E_{comp} - E_m + V_f E_m)/(\alpha V_f) \quad (4)$$

where E_{comp}, E_f ,and E_m are the moduli of the composite, fiber and matrix material, respectively, α is a coefficient associated with fiber orientation, which for 3D randomly oriented fibers is 0.2, and V_f is the volume fraction of MWCNTs calculated from density = mass/volume. As shown in Table I, the E_{comp} values determined using this model are 3 orders of magnitude greater than those measured experimentally. E_{comp} was also calculated using a modified form of the 'rule of mixtures' law, Krenchel's model, where the volume fraction of CNTs (V_{NT}) is now obtained from

$$V_{NT} = \left[\frac{\rho_r}{m_{NT}} - \rho_r + 1\right]^{-1} \quad (5)$$

where $\rho_r = \rho_{NT}/\rho_m$, i.e., the ratio of CNT to matrix density and $\rho_{NT} = 1.3$ g/cm^3. Again, the E_{comp} values obtained were orders of magnitude greater than the experimental values. Finally, we attempted to compare the experimental data with the Halpin-Tsai model adopted for randomly oriented composites given by the expression

$$\frac{Y_c}{Y_m} = \frac{3}{8}\left[\frac{1 + \zeta\eta_L V_f}{1 - \eta_L V_f}\right] + \frac{5}{8}\left[\frac{1 + 2\eta_T V_f}{1 - \eta_T V_f}\right] \quad (6)$$

where

$$\eta_L = \frac{Y_f/Y_m - 1}{Y_f/Y_m + \zeta} \quad (7)$$

and

$$\eta_T = \frac{Y_f/Y_m - 1}{Y_f/Y_m + 2} \quad (8)$$

and Y_c, Y_m, and Y_f are the moduli of the composite, matrix and fiber respectively, V_f is volume fraction of fiber and ζ is a constant shape factor, normally between 1 and 2.[40] As can be seen from Table I, there is relatively poor agreement for the modulus values determined experimentally and using the models based on ''rule of mixtures.'' However, the values calculated using the Halpin-Tsai model provide a better fit, particularly for the high aspect ratio tubes. Similar behavior was obtained irrespective of the nanotube loading, in line with Halpin-Tsai theory for composites having low loadings of filler. The difference between the experimental and theoretical values obtained confirms that stress transfer between carbon nanotubes and the matrix polymer is a complex combination of physical and chemical mechanisms.

Evidence for both mechanisms and strong interactions between polymer chain and nanotube was obtained from Raman spectroscopy studies from the first processing stage in the preparation of the nanocomposites when the diisocynate is mixed with the MWCNTs. Figure 5(a) shows the Raman spectra of the MWCNTs, PU resin, diisocynate and polyol precursors, and precursor/MWCNT solutions in the range 500–3000 cm^{-1}. No changes in the spectrum of the polyol were observed on addition of MWCNTs, in contrast to the spectra of the IPDI/MWCNT mixes which showed two distinct changes. Firstly, one can tentatively assign the peak at 1420 cm^{-1} to the symmetric stretch of the N=C=O functional group of IPDI, which up-shifts significantly by 38 and 42 cm^{-1} (to 1458 and 1462 cm^{-1}) on addition of 0.1 and 1.0 wt % MWCNT respectively. Furthermore, the intensity of this peak is reduced with increasing CNT concentration. Secondly, but less obvious from Figure 5(a) and thus shown more clearly in Figure 5(b), the peak at 766 cm^{-1} assigned to a C—H out-of plane bending vibration mode up-shifted by 14 cm^{-1} and became more broad on addition of just 0.1 wt % MWCNTs. The simultaneous broadening and shifting of these peaks is evidence of the MWCNTs interacting with the IPDI monomer through restriction of its natural molecular motion and strong attractive forces between the N=C=O functional group and polar groups at defect sites along the carbon nanotubes. Upon addi-

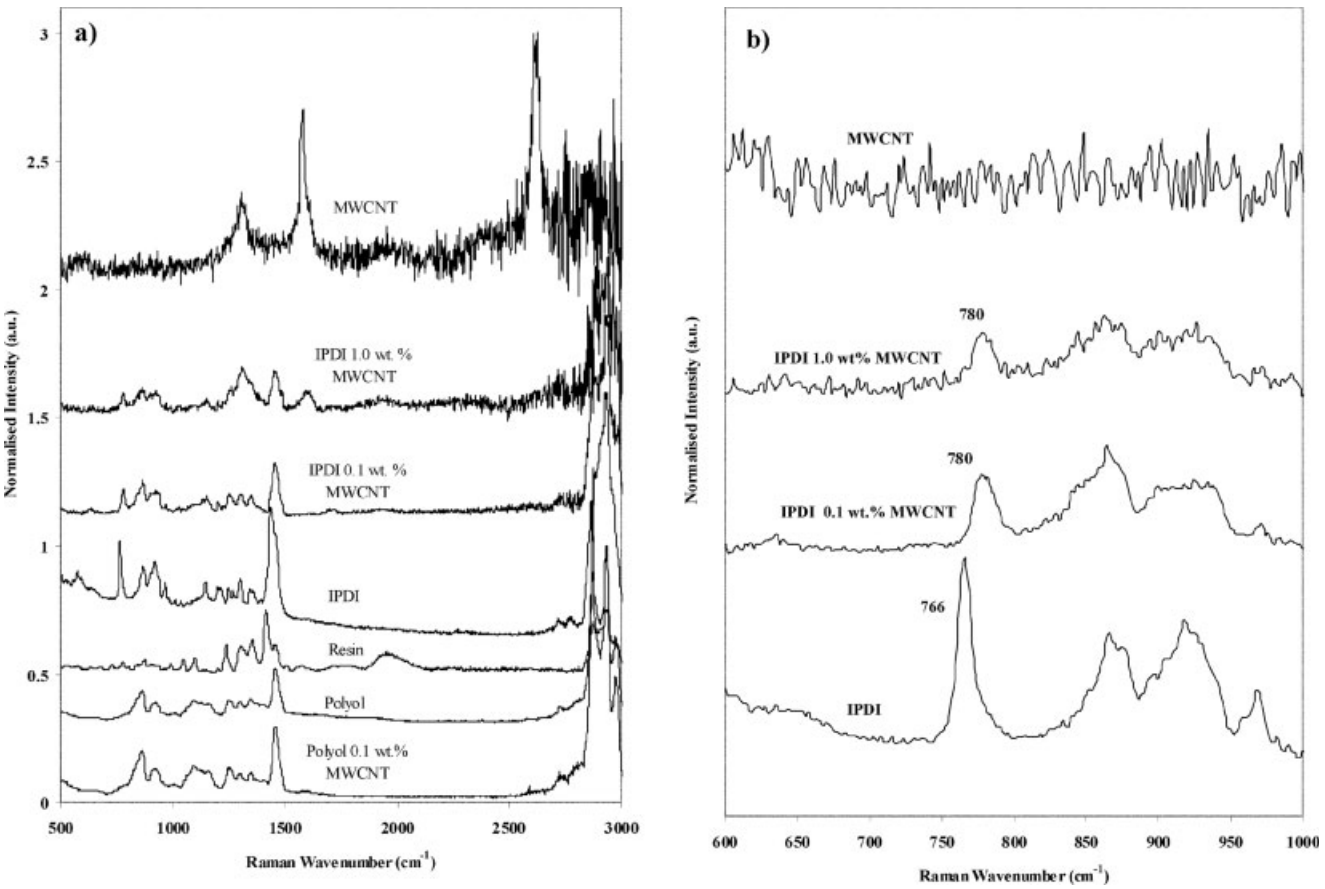

Figure 5 Raman spectra of (a) PU precursors, MWCNTs, precursor mixes with 0.1 wt % nanotubes and PU resin and (b) isophrone diisocynate/MWCNT mixes in the range 600–1000 cm^{-1}.

tion of the polyol and during the curing reaction, the CNTs become intertwined in the 3-D resin network. Under an applied tensile load, the CNTs experience mechanical interlocking and resist detachment from the PU matrix. Xu et al.[26] used such a term to describe a CNT filled epoxy matrix which produced a 20% enhancement in elastic modulus when 0.1 wt % MWCNTs were added.

Figure 6(a) shows the Raman spectra from 250 to 2250 cm^{-1} for the MWCNTs, 0.1 and 1.0 wt % composites and the PU resin. The Raman frequency, intensity and band shape of the vibrations can vary when nanotubes interact with other species. Generally, the interaction between nanotube and polymer is reflected by a peak shift or a peak width change.[37] Significant peak shifting was observed for the peaks assigned the D and G bands of the MWCNTs at 1314 and 1582 cm^{-1} respectively, and are shown in Figure 6(b). The addition of 1.0 wt % MWCNTs to the PU induces an upshift in the tangential mode (G-band) centered at 1582 by 24 cm^{-1} concomitant with the peak broadening. Such behavior has been observed previously by Dieckmann et al.[41] for a peptide/SWCNT composite, which the authors associated with the polymer coating individual nanotubes. This supports our microscopic observations in that a visible adsorbed layer of polymer surrounding the protruding nanotubes with increased diameter was evident, indicating good surface wetting and therefore good interfacial adhesion between the PU and MWCNTs. It is also possible from the Raman data to estimate the compressive strain on the nanotubes because of the shrinkage of the thermosetting polyurethane resin using

$$\Delta\omega^{\pm}/\omega_0 = -\gamma(1 - \nu_\tau)\varepsilon_z \quad (9)$$

where $\Delta\omega^{\pm}/\omega_0$ is the relative shift of the G band (cm^{-1}), γ is known as the Grüneisen parameter which describes the frequency shift under hydrostatic strain and can be approximated to 1.24 for nanotubes,[42] ν is the Poisson ratio and taken to be 0.28[43] and ε_z is the compressive strain. For both the 0.1 and 1.0 wt % PU/MWCNT composites, ε_z was determined to be −1.56%, almost eight time greater than that reported for an epoxy/SWCNT composite but with 5 wt % nanotube loading.

Figure 7(a) shows the storage modulus (E') and (b) tan δ curves of the PU and PU/MWCNT nanocomposites as a function of temperature. The addition of 0.1 wt % MWCNTs resulted in a marked increase of the storage modulus over the entire temperature range

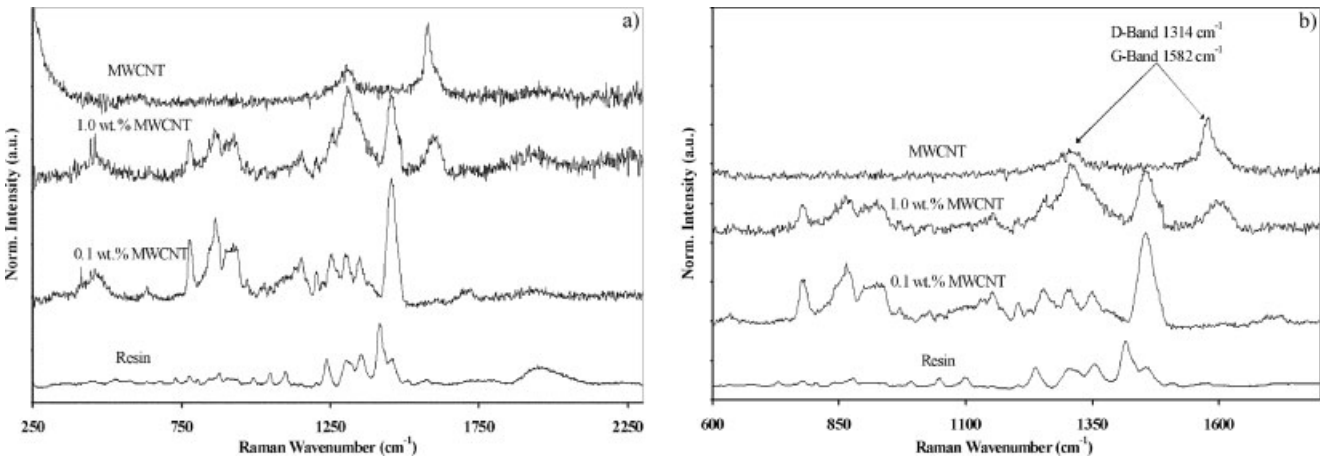

Figure 6 Raman spectra of thermoset PU, MWCNTs, and their composites in the range (a) 250–2300 cm^{-1} and (b) 600–1750 cm^{-1}.

studied. From −60°C to the onset of the T_g the storage modulus of the 0.1 wt % composite was on average 1.3 times larger than the original PU. In the same temperature range the storage modulus of the 1.0 wt % MWCNT composite remained similar to the PU resin until the approach of the T_g. At ~30°C the storage modulus of the 1.0 wt % MWCNT nanocomposite was more than 2.1 times larger than the original value of PU. Above the T_g the storage modulus of both composites begins to plateau and is significantly increased by the presence of MWCNTs, but is greater for the 0.1 wt % composite. That the storage modulus of the composite with the higher loading of MWCNTs is lower is associated with the reduced crosslink density of the cured PU resin and is caused by the MWCNTs altering the stoichiometry of the PU matrix. By convention, the glass transition temperature (T_g, °C) was taken from the peak maxima of the tan δ curves obtained at 1 Hz. Surprisingly, the T_g of the neat resin (41°C) was increased on the addition of 0.1 wt % MWCNTs by 6°C and a further 4°C for the 1.0 wt % composite to 51°C. It may be considered that the presence of MWCNTs hindered the polymer chain mobility within the PU resin, also evident in the Raman results.

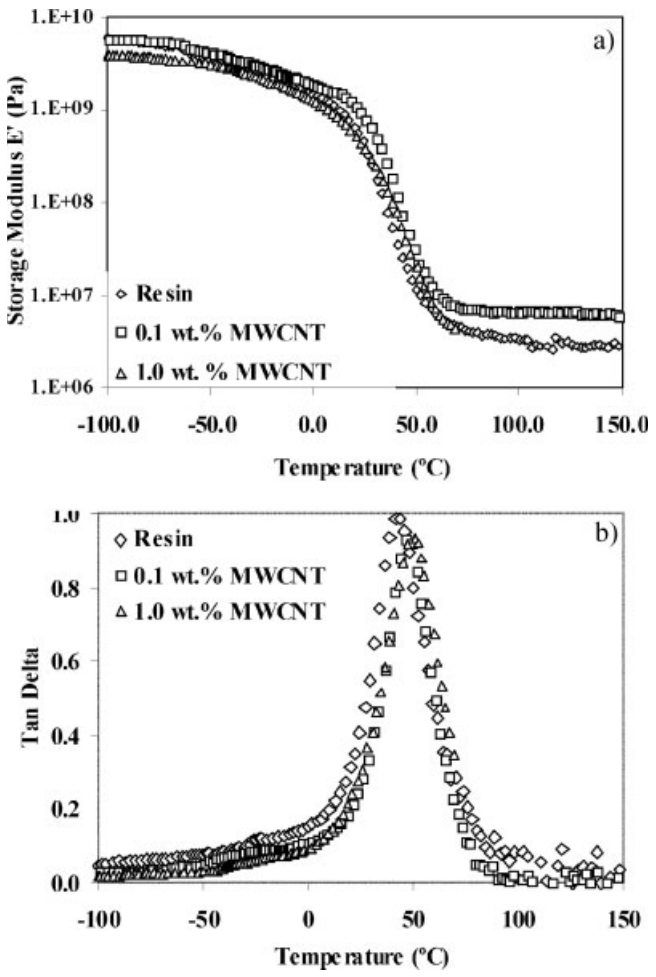

Figure 7 DMA traces for TPU/MWCNT nanocomposites, (a) storage modulus and (b) tan δ as a function of temperature.

CONCLUSIONS

Composites of uniformly dispersed MWCNTs in a thermoset polyurethane, confirmed from SEM, HRTEM and WAXD results, were successfully prepared by adding the nanotubes to the isophrone diisocyanate precursor with high speed shear mixing prior to completing the curing reaction. A true nanoscale reinforcing effect was obtained, in that the stiffness, strength and relative toughness of the PU matrix was greatly enhanced on addition of as little as 0.1 wt % MWCNTs. The Young's modulus, ultimate tensile strength and strain at break increased by 561, 397, and 302% respectively. The modulus of the composites predicted by the Halpin-Tsai model was a good fit with that determined experimentally, but only for high aspect ratio nanotubes and is in agreement with

that predicted by Halpin-Tsai theory. Raman spectroscopy studies on the IPDI/MWCNT mix and the nanocomposites clearly demonstrated that strong interactions exist between the PU matrix and MWCNTs, as a consequence of the significant up-shifting of peaks and reduced peak intensity observed, thus providing the mechanism for stress transfer at the interface between nanotube and polymer that is manifest in the large increases in the mechanical properties obtained. The interfacial shear stress calculated from the modified Kelly-Tyson model and work done to 'pullout a fiber' for this PU/MWCNT system are much greater than that reported for epoxy/CNT systems. The increase in the T_g of the PU resin of up to 10°C on addition of MWCNTs, obtained from DMA measurements, would suggest the mobility of the polymer chains is greatly hindered because of the interactions between PU matrix and nanotubes. It is evident from the above results that these interactions could be both physical and chemical. Interactions such as hydrogen bonding between isocyanate and hydroxyl (—OH) or carboxyl (—COOH) functional groups at defect sites along the carbon nanotube followed by addition of the polyol to complete the curing reaction results in the interlocking of carbon nanotubes at crosslink sites which have a reinforcing effect during tensile deformation.

CMcC thanks Hamilton Erskine Ltd. for funding a studentship, and the authors would like to acknowledge Mr Jackie Stevenson for technical assistance.

References

1. Szleifer, I.; Yerushalmi-Rozen, R. Polymer 2005, 46, 7803.
2. Belin, T.; Epron, F. Mater Sci Eng B 2005, 119, 105.
3. Andrews, R.; Weisenberger, M. C. Curr Opin Solid State Mater Sci 2004, 8, 31.
4. McNally, T.; Pötschke, P.; Halley, P.; Murphy, M.; Martin, D.; Bell, S. E. J.; Brennan, G. P.; Bien, D.; Lemoine, P.; Quinn, J. P. Polymer 2005, 46, 8222.
5. Pötschke, P.; Brünig, H.; Janke, A.; Fischer, D.; Jehnichen, D. Polymer 2005, 46, 10355.
6. Kashiwagi, T.; Du, F.; Winey, K. I.; Groth, K.; Shields, J. Polymer 2005, 46, 471.
7. Miyagawa, H.; Drzal, L. Polymer 2004, 45, 5163.
8. Bhattacharyya, A.; Sreekumar, T.; Liu, T.; Kumar, S.; Ericson, L.; Hauge, R.; Smalley, R. Polymer 2003, 44, 2373.
9. Zilli, D.; Chiliotte, C.; Escobar, M.; Bekeris, V.; Rubiolo, G.; Cukierman, A.; Goyanes, S. Polymer 2005, 46, 6090.
10. Kukovecz, Á.; Kanyó, T.; Kónya, Z.; Kiricsi, I. Carbon 2005, 43, 994.
11. Gong, X.; Liu, J.; Baskaran, S; Voise, R.; Young, J. Chem Mater 2000, 12, 1049.
12. Ruan, S. L.; Gao, P.; Yang, X. G.; Yu, T. X. Polymer 2003, 44, 5643.
13. Jiang, X.; Bin, Y.; Matsuo, M. Polymer 2005, 46, 7418.
14. Sung, J.; Kim, H. S.; Jin, H.; Choi, H. J.; Chin, I. Macromolecules 2004, 37, 9899.
15. Khare, B.; Wilhite, P.; Meyyappan, M. Nanotechnology 2004, 15, 1650.
16. Coleman, J. N.; Khan, U.; Blau, W. J.; Gun'ko, Y. K. Carbon 2006, 44, 1624.
17. Gibson, R. F.; Ayorinde, E. O.; Wen, Y.-F. Compos Sci Technol 2007, 67, 1.
18. Sandler, J. K. W.; Kirk, J. E.; Kinloch, I. A.; Shaffer, M. S. P.; Windle, A. H. Polymer 2003, 44, 5893.
19. Sandler, J. K. W.; Shaffer, M. S. P.; Prasse, T.; Bauhofer, W.; Schulte, K.; Windle, A. H. Polymer 1999, 40, 5967.
20. Martin, C. A.; Sandler, J. K. W.; Shaffer, M. S. P.; Schwarz, M.-K.; Bauhofer, W.; Schulte, K.; Windle, A. H. Compos Sci Technol 2004, 64, 2309.
21. Barrau, S.; Demont, P.; Peigney, A.; Laurent, C.; Lacabanne, C. Macromolecules 2003, 36, 5187.
22. Gojny, F. H.; Wichmann, M. H. G.; Fiedler, B.; Kinloch, I. A.; Bauhofer, W.; Windle, A. H.; Schulte, K. Polymer 2006, 47, 2036.
23. Song, Y. S.; Youn, J. R. Carbon 2005, 43, 1378.
24. Schadler, L.; Giannaris, S.; Ajayan, P. Appl Phys Lett 1998, 73, 3842.
25. Wong, M.; Paramsothy, M.; Xu, X. J.; Ren, Y.; Li, S.; Liao, K. Polymer 2003, 44, 7757.
26. Xu, X.; Thwe, M.; Shearwood, C.; Liao, K. Appl Phys Lett 2002, 81, 2833.
27. Liu, L.; Wagner, H. D. Compos Sci Technol 2005, 65, 1861.
28. Bai, J. B. Carbon 2003, 41, 1325.
29. Bai, J. B. Compos A 2003, 34, 689.
30. Gojny, F. H.; Schulte, K. Compos Sci Technol 2004, 64, 2303.
31. Biercuk, M. J.; Liaguno, M. C.; Radosavljevic, M.; Hyun, J. K.; Johnson, A. T.; Fischer, J. E. Appl Phys Lett 2002, 80, 2767.
32. Martin, C. A.; Sandler, J. K. W.; Windle, A. H.; Schwarz, M.-K.; Bauhofer, W.; Schulte, K.; Shaffer, M. S. P. Polymer 2006, 46, 877.
33. Choi, E. S.; Brooks, J. S.; Eaton, D. L.; Al-Haik, M. S.; Hussaini, M. Y.; Garmestani, H.; Li, D.; Dahmen, K. Appl Phys Lett 2003, 94, 6034.
34. Puglia, D.; Valentini, L.; Kenny, J. M. J Appl Polym Sci 2003, 88, 452.
35. Ogasawara, T.; Ishida, Y.; Ishikawa, T.; Yokota, R. Compos A 2004, 35, 67.
36. Qian, D.; Dickey, E. Appl Phys Lett 2000, 76, 2868.
37. Zhou, O.; Fleming, R. M.; Murphy, D. W.; Chen, C. H.; Haddon, R. C.; Ramirez, A. P. Science 1994, 263, 1744.
38. Wagner, H. D.; Lourie, O.; Feldman, Y.; Tenne, R. Appl Phys Lett 1998, 72, 188.
39. Cooper, C. A.; Cohen, S. R.; Barber, A. H.; Wagner, H. D. Appl Phys Lett 2002, 81, 3873.
40. Desai, A. V.; Haque, M. A. Thin Walled Struct 2005, 43, 1787.
41. Dieckmann, G. R.; Dalton, A. B.; Johnson, P. A.; Razal, J.; Chen, J.; Giordono, G. M.; Munoz, E.; Musselman, I.; Baughman, R. H.; Draper, R. J. J Am Chem Soc 2003, 125, 1770.
42. Reich, S.; Jantoljak, H.; Thomsen, C. Phys Rev B 2000, 61, 389.
43. Lu, J. P. Phys Rev Lett 1997, 79, 1297.